Available online at www.sciencedirect.com
SCIENCE DIRECT
ELSEVIER
Physica E 32 (2006) 93–96
PHYSICA E
www.elsevier.com/locate/physe

Theoretical predictions of the electronic and optical properties of single and coupled (In,Ga)As/GaAs quantum dots

Gustavo A. Narvaez, Lixin He, Gabriel Bester, Alex Zunger*

National Renewable Energy Laboratory, Golden, CO 80401, USA

Available online 17 February 2006

Abstract

We show how an atomistic pseudopotential plus many-body configuration interaction theory can address the main spectroscopic features of self-assembled dots including, excitons, trions, biexcitons, fine-structure, charging spectra as well as electric-field dependence of entanglement in dot molecules.

PACS: 78.67.Hc; 73.21.La; 03.67.Mn; 71.35.Pq; 74.62.Fj

Keywords: Quantum dots; Neutral excitons; Trions; Charging spectroscopy; Entanglement

1. Introduction

Once upon a time, the electronic structure of self-assembled (In,Ga)As/GaAs quantum dots was described via the single-band, particle-in-a-box (EMA) approach [1]. The latter neglects the correct atomistic symmetry, inter-band (Γ_{15v}–Γ_{1c}–Γ_{15c}) and inter-valley (Γ–X) couplings, as well as strain and alloying effects. Later on, a few-band $\mathbf{k}\cdot\mathbf{p}$ approach was adopted [2]. It now appears that these approaches suffer from some degree of "farsightedness" [3] in that their wave-function representation lacks the resolution needed to "see" the correct symmetry [4]. This is evidenced by the fact that these approaches fail to reproduce a *splitting* of the confined "p"-levels, or the fine-structure effects [5] on the neutral exciton in cylindrically-symmetric quantum dots. Farsightedness of EMA and $\mathbf{k}\cdot\mathbf{p}$ models is also responsible for the absence of both lh_1–hh_2 coupling in AlAs/GaAs superlattices and lh_1–hh_1 coupling in InAs/GaSb superlattices [3]. An alternative approach [4] uses an atomistic wave function (via the pseudopotential method) plus configuration interaction (CI) (for many-body effects). Here, we list a few recent advances obtained with this approach.

2. Single (In,Ga)As/GaAs quantum dots

Electronic structure of (In, Ga)As/GaAs quantum dots versus dot height—While electronic and spectroscopic properties of self-assembled (In,Ga)As/GaAs dots depend on their shape, height and alloy compositions, these characteristics are often not known accurately from experiments. This creates a difficulty in comparing measured electronic and spectroscopic properties with calculated ones. We offer to bridge this gap by providing accurately calculated results as a function of the dot height and composition [6]. Our calculations are based on an atomistic pseudopotential approach that naturally includes quantum-confinement effects, but also inter-band, inter-valley, and spin–orbit couplings [4]. We find the following: (i) While the confined *electron* states form shells with a predominant "s", "p", ... orbital character, the confined *hole* does not show a clear shell picture and tends to have a mixed orbital character. (ii) In *alloy* dots, the electrons' "s–p" splitting depends weakly on height, while the "p–p" splitting depends non-monotonically—due to alloy fluctuations. In pure, *non-alloyed* InAs/GaAs dots, *both* these splittings depend weakly on height. Further, the "s–p" splitting is larger while the "p–p" has nearly the same magnitude. For hole states in alloy dots, the "s–p" splitting decreases with increasing height, whereas the "p–p"

*Corresponding author. Fax: +1 303 384 6531.
E-mail address: alex_zunger@nrel.gov (A. Zunger).

1386-9477/$ - see front matter © 2006 Elsevier B.V. All rights reserved.
doi:10.1016/j.physe.2005.12.142

splitting remains nearly unchanged. (iii) As height increases, the "s" and "p" character of the wave function of the highest-energy hole state becomes mixed, and so does the heavy- and light-hole character. (iv) While in alloy dots the wave function of low-lying hole states are localized inside the dot, in non-alloyed InAs/GaAs dots these states become localized at the interface as height increases. The localized states are driven by the inhomogeneous biaxial strain within the dot and are polarized along $[1\,\bar{1}\,0]$ and $[1\,1\,0]$.

Electronic and optical properties of neutral excitons and biexcitons, and trions versus dot height—By using the pseudopotential–CI approach, we have calculated the height dependence of recombination energies, polarization, and radiative lifetimes of the optical transitions of neutral excitons (X^0) and biexcitons (XX^0), and negatively (X^-) and positively charged (X^+) trions in lens-shaped, self-assembled $In_{0.6}Ga_{0.4}As/GaAs$ quantum dots [7]. We find that (i) the recombination energy of the lowest transition of X^- blue-shifts as height increases, whereas that of X^+ red-shifts. Remarkably, the recombination of XX^0 shows a red-shift at small heights, reaches a maximum shift, and then blue-shifts for taller dots. This feature results from the height dependence and relative magnitude of the inter-electronic direct Coulomb interaction. (ii) Changes in dot height lead to a bound-to-unbound crossover for X^-, X^+ and XX^0. (iii) The fine structure of neutral excitons presents a splitting even for symmetric dots [5]. This splitting is enhanced by shape anisotropy. (iv) The lowest transitions of X^0 and XX^0 manifest $[1\,1\,0]$ versus $[1\,\bar{1}\,0]$ in-plane polarization anisotropy. This polarity switches sign as a function of height as well as alloy randomness. This reflects a change of sign of the fine-structure splitting. X^- and X^+ show transitions with negligible polarization anisotropy regardless of height. (v) The ground state of X^0 is split into a low-energy pair that is forbidden (dark) and a high-energy pair that is allowed; thus, at $T = 0\,K$ the radiative lifetime $\tau(X^0)$ is long (~ms) due to the dark exciton. On the other hand, at $T = 10\,K$, $\tau(X^0)$ decreases moderately as height increases and its magnitude ranges from 2–3 ns. The groundstate of X^- and X^+ and that of XX^0 is allowed (bright); so, $\tau(X^-)$, $\tau(X^+)$ and $\tau(XX^0)$ are fast (~ns) even at $T = 0\,K$. These radiative lifetimes depend weakly on height. In addition, $\tau(X^-) \sim \tau(X^+) \simeq 1.1$ ns, while $\tau(XX^0) \simeq 0.5$ ns.

Pressure effects on neutral excitons and biexcitons, and trions—We have predicted the pressure dependence of the binding energies of neutral excitons, biexcitons, and trions in lens-shaped, self-assembled $In_{0.6}Ga_{0.4}As/GaAs$ quantum dots [8]. Namely, (i) with applied pressure the binding energy of X^0 and X^+ increases and that of X^- decreases, whereas the binding energy of XX^0 is nearly pressure independent. (ii) Correlations have a small effect in the binding energy of X^0, whereas they largely determine the binding energy of X^-, X^+ and XX^0. (iii) Correlations depend weakly on pressure; thus, the pressure dependence of the binding energies can be understood within the Hartree–Fock approximation and it is controlled by the pressure dependence of the direct Coulomb integrals J. Thus, our results in (i) can be explained by noting that holes are more localized than electrons, so the Coulomb energies obey $J^{(hh)} > J^{(eh)} > J^{(ee)}$.

Few-hole configurations in hole-charged dots—We have calculated the hole-charging spectra on three-dimensionally confined quantum dots. Unlike the case in real atoms, in self-assembled (In,Ga)As/GaAs quantum dots, the Coulomb repulsion between holes $J^{(hh)} \sim 15$–25 meV is comparable to the single-particle energy spacing $\Delta\varepsilon \sim 10$–$20$ meV between confined hole states. This opens the possibility of observing stable, exotic spin configurations that defy the rules of atomic physics (Hund's rules and Aufbau principle). We predict both electron- and hole-charged states in (In,Ga)As/GaAs self-assembled quantum-dots. We find that while electron charging follows both the Aufbau principle and Hund's rules, hole charging gives rise to stable but unusual spin configurations [9].

Within a two-dimensional (parabolic confinement), effective-mass approximation (2D-EMA) it is possible to relate all the electron and hole Coulomb integrals, respectively, to the "s-"like direct Coulomb integrals $J_{ss}^{(ee)}$ and $J_{ss}^{(hh)}$ on the lowest confined state [11]. However, our atomistic calculation of wave functions [10,6] of both electrons and holes shows that they are not of pure conduction-band character (electron) or heavy-hole, light-hole characters (hole); nor do they have pure "s", "p" angular-momentum characters as predicted by the 2D-EMA model. We find that the relation between Coulomb integrals would be different from what is predicted from the 2D-EMA model. To illustrate the differences, we plot

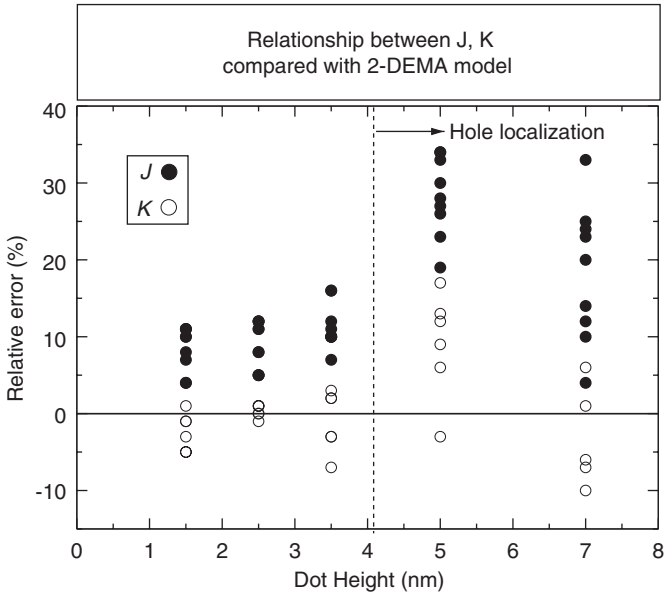

Fig. 1. Relative errors $[J^{(hh)}/J_{ss}^{(hh)}]_{atm} - [J^{(hh)}/J_{ss}^{(hh)}]_{2D}$ (solid circles) and $[K^{(hh)}/J_{ss}^{(hh)}]_{atm} - [K^{(hh)}/J_{ss}^{(hh)}]_{2D}$ (open circles) for holes in lens-shaped non-alloyed InAs/GaAs quantum dots (base diameter $b = 25$ nm). The dashed line shows the region at which interfacial hole localization starts to occur.

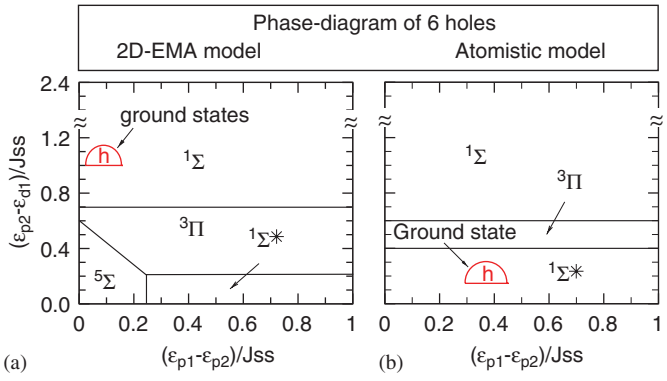

Fig. 2. Phase-diagrams of six holes loaded in non-alloyed InAs/GaAs quantum dots predicted by (a) 2D-EMA model and (b) atomistic model. Phase $^5\Sigma = (s^{\uparrow}s^{\downarrow})(p_1^{\uparrow})(p_2^{\uparrow})(d_1^{\uparrow})(d_2^{\uparrow})$, $^3\Pi = (s^{\uparrow}s^{\downarrow})(p_1^{\uparrow}p_1^{\downarrow})(p_2^{\uparrow})(d_1^{\uparrow})$, $^1\Sigma = (s^{\uparrow}s^{\downarrow})(p_1^{\uparrow}p_1^{\downarrow})(p_2^{\uparrow}p_2^{\downarrow})$, and $^1\Sigma^* = (s^{\uparrow}s^{\downarrow})(p_1^{\uparrow}p_1^{\downarrow})(d_1^{\uparrow}d_1^{\downarrow})$. "h" indicates the ground state.

in Fig. 1 the relative error for hole–hole Coulomb $[J^{(hh)}/J_{ss}^{(hh)}]_{atm} - [J^{(hh)}/J_{ss}^{(hh)}]_{2D}$ and exchange energies $[K^{(hh)}/J_{ss}^{(hh)}]_{atm} - [K^{(hh)}/J_{ss}^{(hh)}]_{2D}$, where "atm" and "2D" means, respectively, atomistically calculated J's and 2D-EMA parabolic values. EMA errors are generally within 20% of $J_{ss}^{(hh)}$ for flat dots. For taller dots, the agreement is worse, and for very tall dots (7 nm), the hole wave functions are localized on the interface of the dot by the strain [10,6]; so, the 2D-EMA model breaks down.

These differences (Fig. 1) are enough to change the hole-charging phase-diagram [9]. In Fig. 2, we compare the phase-diagram of six holes calculated from the atomistic pseudopotential method to those predicted by the 2D-EMA model. We see that the phase boundaries in the atomistic approach are totally different than those of 2D-EMA model. For instance, phase $^5\Sigma = (s^{\uparrow}s^{\downarrow})(p_1^{\uparrow})(p_2^{\uparrow})(d_1^{\uparrow})(d_2^{\uparrow})$ in the 2D-EMA model disappeared in the atomistic approach. In addition, the ground state is now $^1\Sigma^* = (s^{\uparrow}s^{\downarrow})(p_1^{\uparrow}p_1^{\downarrow})(d_1^{\uparrow}d_1^{\downarrow})$ [Fig. 2(b)] instead of $^1\Sigma = (s^{\uparrow}s^{\downarrow})(p_1^{\uparrow}p_1^{\downarrow})(p_2^{\uparrow}p_2^{\downarrow})$ [Fig. 2(a)] predicted by the 2D-EMA model. Note that the true ground state [Fig. 2(b)], phase $^1\Sigma^*$, corresponds to a six-hole configuration that violates both Hund's rules and the Aufbau principle, and accommodates the holes so that the hole energy-level p_2 is left empty while d_1 is fully occupied.

3. Vertically coupled (In,Ga)As/GaAs dot-molecules

Tuning of entanglement by changing the inter-dot separation—We have used our atomistic approach to calculate the excitonic spectrum in a dot molecule made of two (In,Ga)As/GaAs dots [12,13]. We have showed that simplified high-symmetry models commonly used in the literature yield qualitatively erroneous results [12].

At short inter-dot separations (<8 nm), the single-particle physics of the electron states is close to the one of a homonuclear dimer where the orbitals form bonding/antibonding states while the hole states remain localized on one or the other dot. We showed that the hole behavior can

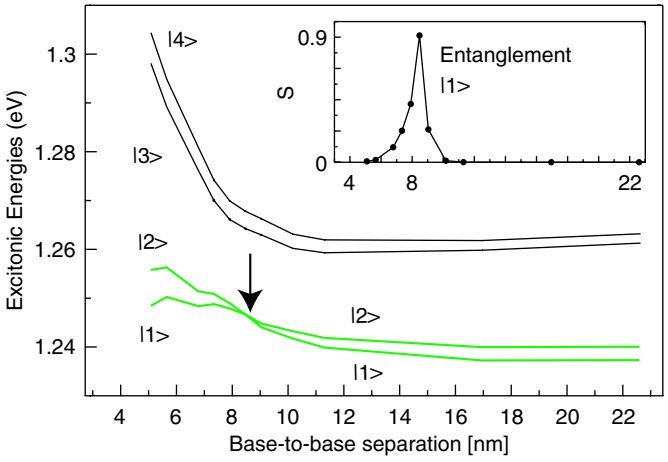

Fig. 3. Energies of the first four exciton states versus dot separation. The inset shows the corresponding degree of entanglement S (see Refs. [12,13] for details).

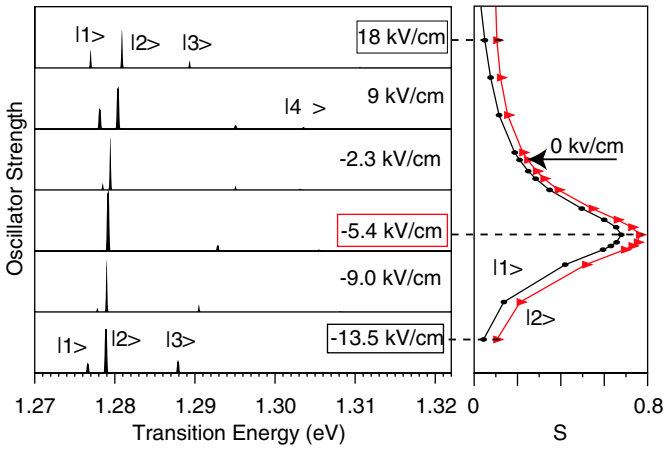

Fig. 4. Oscillator strength of the first four exciton states (left) and S, for states $|1\rangle$ and $|2\rangle$, (right) versus electric field. Dashed lines match the electric field scale of both panels.

be explained by (i) strain, which inhibits inter-dot tunneling, and (ii) the lack of inversion symmetry between self-assembled quantum dots.

Fig. 3 shows the excitonic energies as a function of inter-dot separation and the inset shows the corresponding degree of entanglement of the lowest energy exciton. At large inter-dot separation, both electron and hole behave like a heteronuclear molecule forming two bright (low energy) and two dark (higher energy) excitonic states, all four unentangled. At a critical inter-dot distance of 8.5 nm (arrow in Fig. 3) we predict an anti-crossing of the two bright excitons accompanied by a high degree of entanglement (~80%). We show that the lowest-energy state is antisymmetric and therefore optically dark.

Tuning of entanglement by applying an electric field—As stated above, electron–hole entanglement in two-dot molecules is generally low and develops a sharp maximum only at a specific inter-dot separation that critically depends on the size difference of the two dots. Unfortunately, it has proven to be difficult to experimentally

control precisely the inter-dot distance and the size difference of the two dots. The question we address here is whether the degree of entanglement can be maximized by applying an external electric field in the growth direction. Recently, the use of electric field has been demonstrated in single quantum-dot molecules by Krenner et al. [14]. Fig. 4 shows the oscillator strength of the first four optical transitions as a function of inter-dot separation and the corresponding degree of entanglement. We predict that while the entanglement at zero field is generally low (35% in our case) it can reach a high value (75% in our case) at a specific electric field F_{Smax} ($-5.4\,\mathrm{kV/cm}$ in our case) [15]. Moreover, precisely at this field the first two exciton lines merge, giving a well-defined spectroscopic signature of the point of maximum entanglement.

Acknowledgment

This work was funded by U.S. DOE-SC-BES-DMS, under contract DE-AC3699GO10337 to NREL.

References

[1] L. Jacak, P. Hawrylak, A. Wójs, Quantum Dots, Springer, Berlin, 1998.
[2] D. Bimberg, M. Grundmann, N.N. Ledentsov, Quantum Dots Heterostructures, Wiley, New York, 1999.
[3] A. Zunger, Phys. Stat. Sol. (A) 190 (2002) 467.
[4] A. Zunger, Phys. Stat. Sol. (B) 224 (2001) 727.
[5] G. Bester, S.V. Nair, A. Zunger, Phys. Rev. B 67 (2003) 161306.
[6] G.A. Narvaez, G. Bester, A. Zunger, J. Appl. Phys. 98 (2005) 043708.
[7] G.A. Narvaez, G. Bester, A. Zunger, Phys. Rev. B 72 (2005) 245318.
[8] G.A. Narvaez, G. Bester, A. Zunger, Phys. Rev. B 72 (2005) 041307(R).
[9] L. He, G. Bester, A. Zunger, Phys. Rev. Lett. 95 (2005) 246804.
[10] L. He, G. Bester, A. Zunger, Phys. Rev. B 70 (2004) 235316.
[11] R.J. Warburton, et al., Phys. Rev. B 58 (1998) 16221.
[12] G. Bester, J. Shumway, A. Zunger, Phys. Rev. Lett. 93 (2004) 047401.
[13] G. Bester, A. Zunger, J. Shumway, Phys. Rev. B 71 (2005) 075325.
[14] H.J. Krenner, et al., Phys. Rev. Lett. 94 (2005) 057402.
[15] G. Bester, A. Zunger, Phys. Rev. B 72 (2005) 165334.